Epilepsy Detection from Multi-Channel EEG Using Cross-Recurrence Quantification Analysis and Machine Learning

Nikolaos Mouzakitis

September 24, 2025

Introduction

Recurrence Quantification Analysis (RQA) and Cross-Recurrence Quantification Analysis (CRQA) are nonlinear methods for the analysis of nonstationary time series. The offer the quantification of the recurring patterns in phase space trajectories [19, 20]. Introduced by Trulla et al.[19] (directly built on quantifying recurrence plots[24]) and expanded by Webber and Zbilut[20], RQA measures metrics like recurrence rate, determinism, and laminarity to capture dynamic system behavior. Thomasson et al.[21] in their work, demonstrated RQA's applicability on EEG data, mentioning the robustness it shows in accordance to noise and nonstationarity. Marwan et al.[22] further advanced recurrence plot techniques, emphasizing on developing a confidence measure of RQA in detecting dynamic transitions. Works like these, serve as a foundation of applying RQA and CRQA on EEG studies in various conditions such as epilepsy, cognitive disorders and more as explored in this review.

1 Related Work

Frolov et al.[1] proposed an approach to analyze frequency based multiplex brain networks using recurrence quantification analysis (RQA) on EEG data, and demonstrated the way that recurrence-based synchronization indices can effectively capture both within-frequency (intralayer) and cross-frequency (interlayer) functional connectivity during cognitive tasks. Their work showed that RQA is particularly suitable for analyzing non-stationary EEG signals and revealed important insights about the evolution of functional connectivity patterns during cognitive tasks. In addition the dataset used in this research are openly available in a Figshare repository.

Núñez et al. [16] worked with resting-state EEG recordings from subjects with mild cognitive impairment(MCI), Alzheimer's disease(AD), and healthy ground truth controls in order to detect frequency based changes into their

brain dynamics. By blending wavelet based Kullback–Leibler divergence (KLD) for capturing non-stationarity, and two RQA metrics(*entropy of the recurrence point density* and the *median of the recurrence point density*) insights have been extracted related to neurodegeneration presence. Research's findings show that MCI and AD are presenting notable changes in the recurrence structure and non-stationarity of EEG signals, and more specifics on the theta and beta frequency bands. Therefore, recurrence based dynamics show a capability as potential biomarkers for monitoring and detecting early Alzheimer's disease and its progression.

MCI has also investigated by Timothy et al.[25], where researchers have focused on the classification of MCI using EEG signals and combining RQA and CRQA methods. Analysis has been performed on both resting-state (eyes closed) and task-based (short-term memory) EEG data, focusing on complexity (via RQA) and synchronization (via CRQA) features. Their results indicate that MCI patients exhibit lower complexity and higher inter- and intra-hemispheric synchronization compared to healthy controls, particularly during memory tasks. The study also proposes a novel feature space approach using RQA and CRQA measures, achieving high classification accuracy (91.7%) under task conditions.

Fan and Chou [15] have also proposed an approach for real-time epileptic seizure detection using as a method the analysis of temporal synchronization patterns of EEG signals with recurrence networks and spectral graph theory. Recurrence plots were used for the modeling of the EEG dynamics, extracting graph theory's features for quantifying the synchronization. Results showed high sensitivity of 98.48% and low latency (6 seconds) for detecting seizure on the CHB-MIT dataset, performing better than other RQA measures.

Heunis and co-authors[23] have utilized resting state EEG and RQA in order to distinguish individuals of ages 0-18 of two categories; ASD(autism spectrum disorder) and typically developing. RQA features were extracted and tested on various linear and nonlinear classifiers achieving 92.9% classification accuracy with nonlinear SVM classifier.

Author in [6], investigated changes related to aging in brain sensorimotor systems using RQA and theta-band functional connectivity in EEG signals. In the study a VR experimental paradigm was utilized with auditory stimulus across different age groups(young and elder subjects). Key findings include that elder subjects present decreased EEG complexity during motor preparation stages as measured by RQA metrics (ΔRR and ΔRTE), and had increased theta band functional connectivity highlighting the potential of RQA in detecting age related biomarkers that were not detectable using standalone signal spectral analysis.

Guglielmo et al. [7] utilized RQA features extracted by EEG signals for the purpose of classification of cognitive performance during mental arithmetic tasks. They used frontal and parietal EEG signals and analyzed them, from 36 participants by extracting six RQA metrics (*recurrence rate, determinism, laminarity, entropy, maximum diagonal line length and average diagonal line length*) from four electrodes (F7, Pz, P4, Fp1). Afterwards by applying machine

learning classifiers (SVM, Random Forest, and Gradient Boosting) and they reached accuracy of classification above 0.85, showing the potential that RQA holds for generalizing on nonlinear dynamics.

Mihajlović [33] studied the discriminative effiency of traditional spectral features in comparisson to RQA-derived nonlinear metrics for the cognitive effort classification purposes. Utilizing a 4-channel wearable EEG headset, data was recorded while subjects perform tasks having variable cognitive load such as relaxation, math, reading. The key finding was that while spectral features alone often yielded higher classification accuracy, RQA features such *recurrence rate,determinism ratio* were consistently ranked among the most important features for discrimination task. A conjuction of a hybrid model using both spectral and RQA features achieved the best overall performance, showing the complementary nature of the methods in brain dynamics exploration.

Yang and co-authors [17], examined stereo electroencephalography (sEEG) recordings of 10 patients with refractory focal epilepsy for analyzing dynamical differences among discreet epileptic phases/states (inter-ictal, pre-ictal, and ictal) and regions. Using recurrence plots and CRQA, they identified epileptogenic channels with longer diagonal structures in RPs, which is a sign of more deterministic and recurrent dynamics. Their findings point out that the synchronization among the epileptogenic channels strengthened while seizures events occur, suggesting that these regions dominate the network's dynamics.

Lopes et al. [8] have proposed a combinatorial framework by mixing RQA with dynamic functional network (dFN) analysis, applying it to both MEG and stereo EEG data. The methodology they described is split into five steps: data segmentation, functional network inference, distance computation alongside networks, recurrence plot construction and finally RQA. The study demonstrated that functional networks in epilepsy patients recur more quickly than in healthy controls, suggesting RQA on dFNs could play the role of a potential biomarker. For the EEG dataset investigation, they have showed that the pre-ictal networks shown higher recurrence rates than post-ictal periods, with the τ-recurrence rate (RR_τ) proving particularly effective for seizure detection.

Rangaprakash [18] have proposed an application of RQA for the study of brain connectivity using multichannel EEG signals. In its work, a new CRQA-based feature was proposed (Correlation between Probabilities of Recurrence (CPR)), a nonlinear and non-parametric phase synchronization technique. Afterwards it was utilized for the analysis of functional connectivity in epilepsy subjects during eyes-open/eyes-closed conditions. The results demonstrated that CPR outperformed other known traditional linear methods on distinguishing seizure and pre-seizure states, identifying epileptic foci, and differentiating alongside eyes-open and eyes-closed conditions.

In another study which demonstrates the effectiveness of RQA in analyzing EEG signals for epilepsy detection, Gruszczyńska et al.[11] applied RQA on such signals in order to distinguish epileptic from healthy patients using recordings from frontal and temporal lobe electrodes (Fp1, Fp2, T3, T4). In their findings they have showed that the epileptic signals present more periodic dynamics in comparison to healthy controls, by producing higher values of RQA parameters

3

such as determinism, laminarity, and longest diagonal line. The combination of RQA with Principal Component Analysis for dimensionality reduction and visualization, achieved 86.8% classification accuracy with SVM. Authors also demonstrated RQA's capability to identify pathological patterns in EEG signals without the requirement of seizure events during recording which have bad impact on the subject's health.

Another study utilizing advanced nonlinear analysis techniques for neural correlation investigation to cognitive functions [12] used *stereoelectroencephalography (sEEG)* combined alongside RQA for the examination of the relationship of the DMN and empathy. Correlations have been detected relating specific RQA metrics (mean diagonal line length, entropy of diagonal line lengths, trapping time) and empathy scores, particularly within DMN subsystems.

Regarding epilepsy diagnosis, authors in [13] proposed a new framework utilizing the combintation of RQA with genetic algorithms and Bayesian classifiers for identifying corresponding biomarkers for seizure detection. They utilized five distance norms (e.g., Euclidean, Mahalanobis) and multiple thresholds for extracting recurrence features from EEG signals, achieving 100% classification accuracy. More specific, the *transitivity* feature has shown capability of a highly discriminative biomarker, performing better compared to traditional linear methods.

Ngamga et al.[14] studied the performance achieved of RQA and Recurrence Network (RN) measures in identifying pre-seizure states from multi-day, multi-channel intracranial EEG (iEEG) recordings of epilepsy patients. Results highlighted the correlation among RQA measures (determinism, laminarity, and mean recurrence time) in detecting seizure precursors, while RN measures (average shortest path length and network transitivity) provided complementary but not so consistent insights than using the application of RQA measures alone.

Researchers in [3], have applied RQA on resting-state fMRI data from TgF344-AD rats(a transgenic rat model which will eventually develop Alzheimer's disease) and their healthy-control counterparts wild-type rats(WT), in order to detect early stage biomarkers for the disease. By analyzing Default Mode-Like Network (DMLN) using RQA metrics(*entropy, recurrence rate, determinism and average diagonal line length*) changes have been detected in regions of the basal forebrain, hippocampal fields (CA1, CA3), and visual cortices (V1, V2). Also on the study's findings include reduced predictability in WT rats with aging, while AD rats exhibited less decline in predictability, suggesting some unknown yet countereacting mechanisms. This study highlights RQA's sensitivity for nonlinear dynamics in preclinical AD and the code used is also publicly available.

Lombardi et al.[5] investigated the nonlinear properties in fMRI BOLD signals during a working memory task in schizophrenic patients and healthy controls. They have attempted by using RQA, to analyze recurrence plots for quantifying determinism, trapping time, and maximal vertical line length in functionally relevant brain clusters. Outcome revealed differences in the dynamics between the two groups, and more specific in working memory and DMN areas. While their work have focused on fMRI, the methodology can be

4

adapted also into EEG signals, which can offer a higher resolution for capturing rapid neural dynamics.

Kang et al. [2], in their study explore the dynamics and functional connectivity of the Default Mode Network (DMN) in schizophrenia, applying RQA-CRQA on resting-state fMRI data. Findings include decreased *determinism* between specific DMN regions (vMPFC-posterios cingulate and vMPFC-precuneus) in first-episode schizophrenia patients, as a signal of disturbed predictability of functional interactions. Moreover, their results achieve to correctly classify using SVM(support vector machine) schizophrenia patients from healthy controls with 77% classification accuracy.

In their research, Pentari et al.[9] have applied CRQA to resting-state fMRI data for examining the dynamic functional connectivity on patients with neuropsychiatric systemic lupus erythematosus (NPSLE). Results contain the fact that CRQA metrics, such as determinism, appear more sensitive than conventional static functional connectivity methods in order to identify aberrant connectivity patterns that correlated with visuomotor performance. The study focused on 16 frontoparietal regions and found that CRQA could detect both increased and decreased connectivity in NPSLE patients compared against the healthy controls. Building on these findings, Pentari et al.[10] subsequently expanded the investigation to whole brain network analysis in a larger cohort. In this study they demonstrate the capability of CRQA to integrate multiple recurrence metrics for revealing both hyperconnectivity in parietal regions (angular gyrus and superior parietal lobule) and hypoconnectivity in medial temporal structures (hippocampus and amygdala).

In addition there have been works where simulated data have been used in conjunction with RQA. Lameu et al.[4], investigated burst phase synchronization in neural networks using RQA. They analyzed two network types; a small-world network and a network of networks (to mimic better the real human brain), using coupled Rulkov maps to model bursting neurons. By applying RQA, they identified synchronized neuron groups and quantified their sizes during synchronization transitions. The study showed that RQA measures (*recurrence rate, laminarity inspired*(custom feature)*, and average structure size*) complement traditional order parameters by revealing localized synchronization patterns, such as the formation and growth of synchronized clusters. Kashyap and Keilholz[26] conducted a comprehensive comparison between simulated brain network models (BNMs) and real rs-fMRI data using dynamic analysis techniques, including Recurrence Quantification Analysis (RQA). In the study they employed two BNMs, the Kuramoto oscillator model and the Firing Rate model, for simulating the whole-brain activity, which was then compared to human rs-fMRI data. Among the compared dynamic analysis methods, RQA was proved particularly effective in distinguishing between the models and empirical data, demonstrating that RQA metrics (*recurrence rate, entropy, and average diagonal length*) could robustly separate the empirical data from simulations.

Shalbaf et al. [28] investigated the synchronization of EEG signals between frontal and temporal regions during propofol anesthesia using *Order Patterns*

Cross Recurrence Analysis (OPCR). Their study introduced a novel index, *Order Pattern Laminarity* (OPL), for the quantification of neuronal synchronization and compared its performance with the traditional Bispectral Index (BIS). The results demonstrated that OPL correlated more strongly with propofol concentration ($P_k = 0.9$) and exhibited faster response times to transient changes in consciousness compared to BIS. Additionally, OPL showed lower variability at the point of loss of consciousness (LOC), suggesting its robustness as a measure of anesthetic depth. This work highlights the potential of recurrence-based methods (e.g., CRQA) for analyzing brain network dynamics under anesthesia, particularly in noisy, non-stationary EEG data.

Table 1: Comparison among the retrieved studies using recurrence analysis

#	Reference	Modality	Analysis Methods	Network Type
1	Frolov et al. (2020)	EEG	RQA, CRQA	Multiplex functional networks
2	Kang el al. (2023)	fMRI	RQA, CRQA	DMN, schizophrenia
3	Rezaei el al. (2023)	fMRI	RQA	Default model-like network, AD
4	Lameu et al. (2018)	—	RQA	Small-world & cluster network
5	Lombardi et al. (2014)	fMRI	RQA	schizophrenia,working memory
6	Pitsik E. (2025)	EEG	RQA	aging
7	Guglielmo et al. (2022)	EEG	RQA	cognitive tasks
8	Lopes et al. (2020)	sEEG, MEG	RQA	epilepsy
9	Pentari et al. (2022)	fMRI	RQA, CRQA	NPSLE
10	Pentari et al. (2023)	fMRI	CRQA	NPSLE
11	Gruszczyńska et al. (2019)	EEG	RQA	epilepsy
12	Mo et al. (2022)	sEEG	RQA	DMN, epilepsy
13	Palanisamy et al. (2024)	EEG	RQA	epilepsy
14	Ngamga et al. (2016)	EEG	RQA,RN	epilepsy
15	Fan and Chou (2019)	EEG	RQA,RN	epilepsy, seizure detection
16	Nunez et al. (2020)	EEG	RQA	AD
17	Yang et al. (2019)	sEEG	RQA,CRQA	epilepsy
18	Rangaprakash (2014)	EEG	CPR(CRQA-based)	epilepsy
19	Heunis et al. (2018)	rsEEG	RQA	autism spectrum disorder
20	Timothy et al. (2017)	EEG	RQA-CRQA	MCI
21	Kashyap et al. (2019)	fMRI	RQA	distinguish BNMs
22	Shalbaf et al. (2014)	EEG	CRQA(OPL)	Anesthesia depth monitoring
23	Mihajlović. (2019)	EEG	RQA	cognitive tasks

1.1 RQA relevant patents utilizing EEG modality

The application of RQA on biomedical field related to EEG data, has gathered significant interest, not only in academic research but also in commercial and clinical applications, as evidenced by recent patent filings. These documents can reveal the cutting-edge, industrially viable solutions being developed for

real-time, embedded systems.

Patent US20250195894A1 [39], entitled "Systems and Methods for Seizure Detection and Closed-Loop Neurostimulation," provides a view of the current challenges and proposes a solution for implementing RQA in a resource-constrained environment. Inventors proceed in an alternative calculation of RQA measures which entirely bypass the construction of the recurrence plot matrix(RP). They achieve this, by not creating the traditional RP in order to derive metrics from, but by calculating the RQA metrics *on-the-fly*; dynamically accumulating the lengths of diagonal lines (chains of recurrent points) as each new data point is processed. This method offers two significant advantages:

1. **Memory Efficiency:** It eliminates the need for the large $N \times N$ comparison matrix, reducing memory usage by approximately 88%.

2. **Computational Efficiency:** It avoids the expensive read/write cycles associated with managing the large matrix, reducing processing time by approximately 30% per channel.

In addition, the patent by [40], titled "An EEG signal classification model based on genetic algorithm and random forest", presents a framework for EEG signal classification. The inventors propose a hybrid model consisting of three key stages:

1. **Feature Extraction:** The method employs a multi-modal feature extraction strategy. Among other features, it explicitly includes RQA metrics from the EEG signal, alongside other traditional time-domain/frequency features.

2. **Feature Optimization:** A genetic algorithm (GA) is then utilized for feature selection. Inventors use binary encoding for representing chromosomes, where each bit corresponds to the selection (1) or rejection (0) of a specific feature from the large extracted pool. The aim of this procedure is to optimize the feature subset in order to have maximum discriminative power.

3. **Classification:** The optimized feature subset is fed into a Random Forest classifier for a final prediction.

The patent claims that this integrated approach, validated on a public dataset, yields a superior classification accuracy compared to existing methods at the time of filing, while also demonstrating robustness through cross-validation.

Another patent[41] (CN106512206B) describes an implantable closed-loop deep brain stimulation (DBS) system that uses electrophysiological signals (specific deep brain local field potentials (LFPs) and ECG signals) for monitoring the states of a human sleeping and adjusting various stimulation parameters in real time. A device acquires ECG and deep brain signals for feature extraction in the domains of time and frequency, while calculating complexity measures.

7

RQA metrics such recurrence rate, determinism, entropy and laminarity are utilized alongside other complexity and spectral features to classify sleep states and trigger appropriate stimulation responses. Features are then utilized for detection of sleep stages and for emergency detection/alerts (f.e, cardiac arrest or abnormal excitation).

2 Filtering

Electroencephalogram signals in most cases are contaminated by noise and artifacts from physiological (eye blinks, muscle or cardiac activity) and non-physiological sources (powerline interference). In general, artifacts consist of all the non-neural signals that contaminate the recorded EEG data.

Preprocessing is required in order to increase the quality of the signal(signal-to-noise) for boosting further analysis in various application domains like brain-computer interfaces (BCIs) or clinical diagnostics [29-32].

Common preprocessing techniques include:

- **Filtering** (e.g., Butterworth, Chebyshev) to remove unwanted frequency bands.

- **Regression methods** for correcting ocular artifacts using reference channels.

- **Blind Source Separation (BSS)** (e.g., ICA, CCA) to decompose and isolate neural activity from artifacts.

- **Wavelet/EMD-based methods** for non-stationary artifact removal.

Also hybrid approaches (e.g., wavelet-ICA) combine multiple techniques for improved artifact rejection. The choice of method depends on computational constraints, artifact type, and real-time processing needs. Effective preprocessing is a key that ensures reliable feature extraction for later analysis.

2.1 Evaluation metrics for EEG denoising in the CHB-MIT dataset

In order to evaluate the performance of different wavelet-based filters for EEG denoising, quantitative metrics have been computed over entire recordings per channel and filter configuration. Metrics used were:

- **Signal-to-Noise Ratio (SNR, dB)**: Measures the ratio between the power of the clean signal and the power of the noise. Higher values indicate better noise suppression while preserving the structure of the signal.

- **Root Mean Square Error (RMSE, μV)**: This metric quantifies the average deviation between the denoised and reference signals in microvolts. Lower values indicate closer similarity to the original signal.

- **Normalized RMSE (NRMSE, %)**: RMSE normalized by the dynamic range of the reference signal, expressed as a percentage. Lower values represent better performance.

- **Correlation Coefficient**: Pearson's correlation between the denoised and reference signals, assessing how similar the two compared waveforms are. Values close to 1 indicate high waveform preservation.

9

- **Percent Root-mean-square Difference (PRD, %)**: Measures the relative distortion introduced by the denoising process. Lower values indicate less distortion.

For each one of the filters configuration, metrics were computed channel-wise and then averaged across all channels in order to calculate their global performance score.

2.2 Filter Selection Criteria

The selection of the optimal filter was based on a multi-criteria ranking strategy, where:

1. Metrics where *higher* values indicate better performance (**SNR**, **Correlation**) were ranked in descending order.

2. Metrics where *lower* values indicate better performance (**RMSE**, **NRMSE**, **PRD**) were ranked in ascending order.

3. The ranks from all metrics were averaged to obtain an overall performance rank for each filter.

The filter with the lowest average rank was considered the best compromise between noise reduction and signal fidelity. According to this evaluation, the **SYM8, level 4, threshold 0.5, hard thresholding** filter presented the highest overall performance, exhibiting:

- the highest SNR values,

- one of the lowest RMSE and the lowest NRMSE value,

- the highest correlation coefficient,

- and the lowest PRD.

This indicates that the chosen filter effectively suppressed noise while preserving the morphological features of the EEG signal, making it the most suitable choice for subsequent analysis. The results of the benchmarking those metrics in 5 EDF recording files which include seizures are presented in the following figure.

In the following figures we present a visualization using the recording named *chb01_03.edf* comparing the original 10 first EEG channels against the filtered ones with the respective wavelets filters.

Figure 1: The top 10 filter configurations per EEG metric. RMSE values scaled.

Figure 2

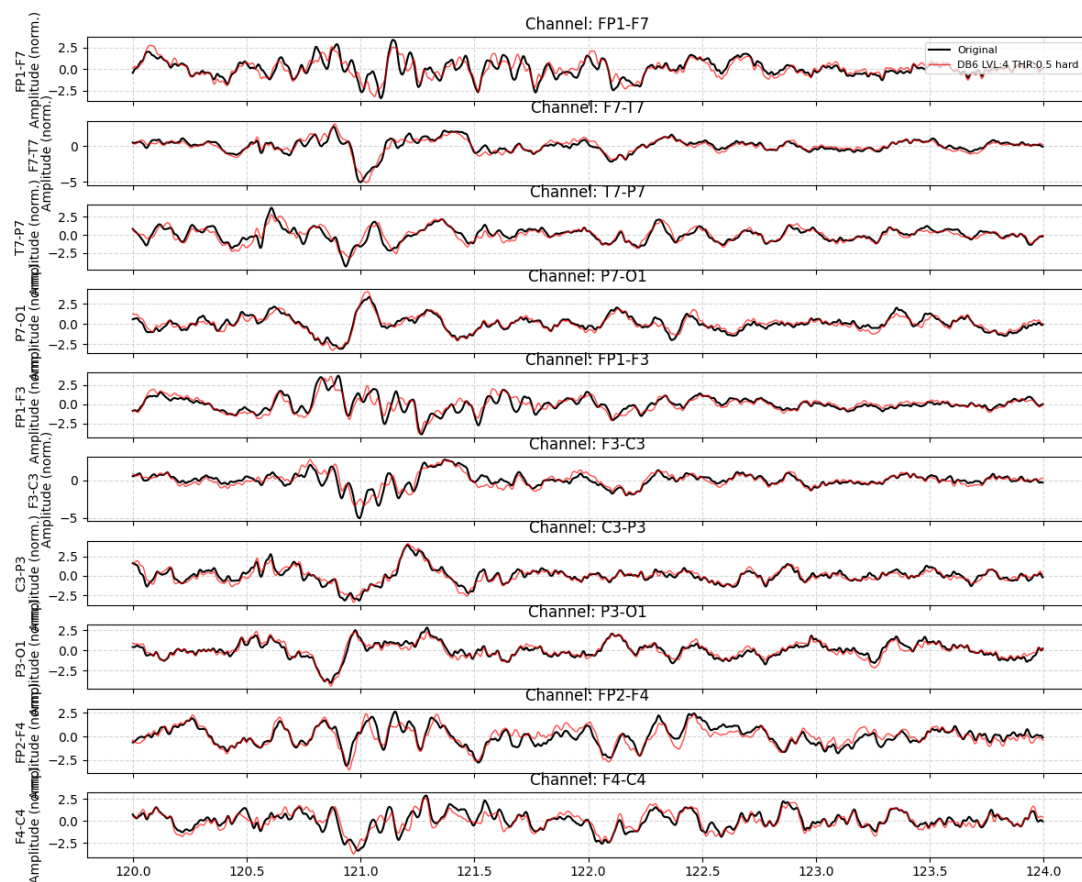EEG Signal Comparison: Original vs. DB6 LVL:4 THR:0.5 hard (chb01_03.edf)

Figure 3

3 Phase space reconstruction of EEG signals

The analysis of nonlinear dynamical systems from experimental time series, such as EEG recordings, requires the reconstruction of the underlying phase space from the scalar measurements of each channel. According to Takens' embedding theorem [34], a time series $x(t)$ can be embedded in an m-dimensional space using time-delay coordinates:

$$\vec{y}(t) = [x(t), x(t+\tau), x(t+2\tau), \ldots, x(t+(m-1)\tau)] \tag{1}$$

where m is the embedding dimension and τ is the time delay. The critical challenge lies in determining the appropriate values for these parameters to faithfully reconstruct the system's dynamics without distortion.

3.1 Determination of Embedding Parameters

The reconstruction of the phase space from a single time series $x(t)$ requires the specification of two parameters: the time delay τ and the embedding dimension m. These two parameters determine how the reconstruction will represent and how close it will reveal the underlying dynamics without distortion.
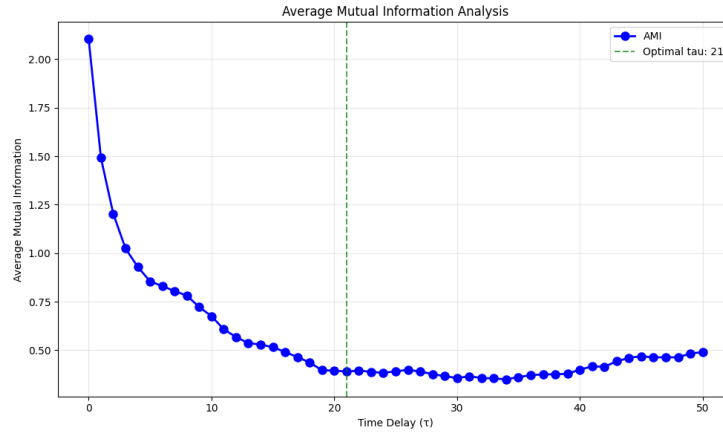

Figure 4: Calculation of τ using AMI for a sample EEG channel. The first minimum of the AMI function (green dashed line) is chosen to become the optimal τ to ensure independence between delay coordinates.

3.1.1 Calculation of time delay τ utilizing mutual information

The time delay τ can be estimated by applying the *Average Mutual Information* (AMI) method, a concept which was first introduced by Fraser and Swinney [36]. In contrast to linear autocorrelation, mutual information has the ability to capture both linear and nonlinear dependencies among the original time series $x(t)$ and its delayed version $x(t+\tau)$.

The mutual information $I(\tau)$ between $x(t)$ and $x(t+\tau)$ is defined as:

$$I(\tau) = \sum_{x(t),\,x(t+\tau)} P(x(t), x(t+\tau)) \, \log_2 \left(\frac{P(x(t), x(t+\tau))}{P(x(t)) \, P(x(t+\tau))} \right)$$

where $P(\cdot)$ denotes probability.

The optimal time delay τ is chosen as the value at which $I(\tau)$ reaches its *first minimum*. This value indicates a good compromise between independence (too small τ) and irrelevance (too large τ) of the coordinates in the embedding vector.

3.1.2 Estimating embedding dimension m using false nearest neighbors approach

When the embedding dimension m is too small, the phase space becomes *projected* rather than properly *embedded*. This projection can create artificial neighborhoods where points appear to be close due to geometrical constraints of the space rather than their actual dynamical similarity. These are named as *false nearest neighbors* [35].
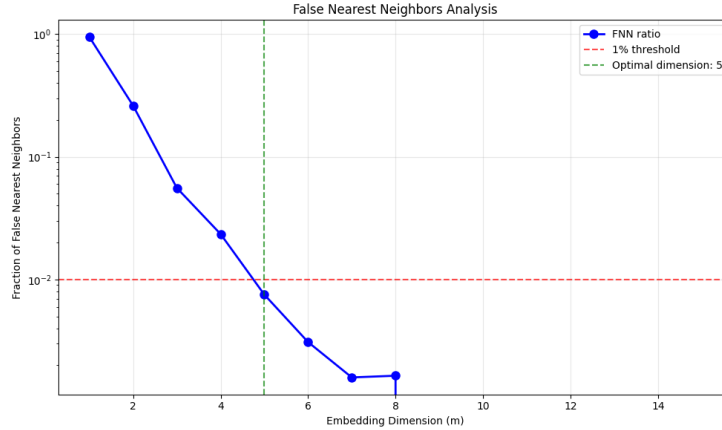

Figure 5: Calculation of the embedding dimension using the FNN scheme.

Mathematically, two points $\vec{y}_i$ and $\vec{y}_j$ are false neighbors if their distance increases significantly when embedded in higher dimension:

$$\frac{\|\vec{y}_i^{(m+1)} - \vec{y}_j^{(m+1)}\|}{\|\vec{y}_i^{(m)} - \vec{y}_j^{(m)}\|} > R_{\text{tol}} \tag{2}$$

where R_{tol} is a tolerance threshold (typically 10–15).

The False Nearest Neighbors(FNN) method [35] provides a systematic approach in order to determine the minimal sufficient embedding dimension. The method's steps are:
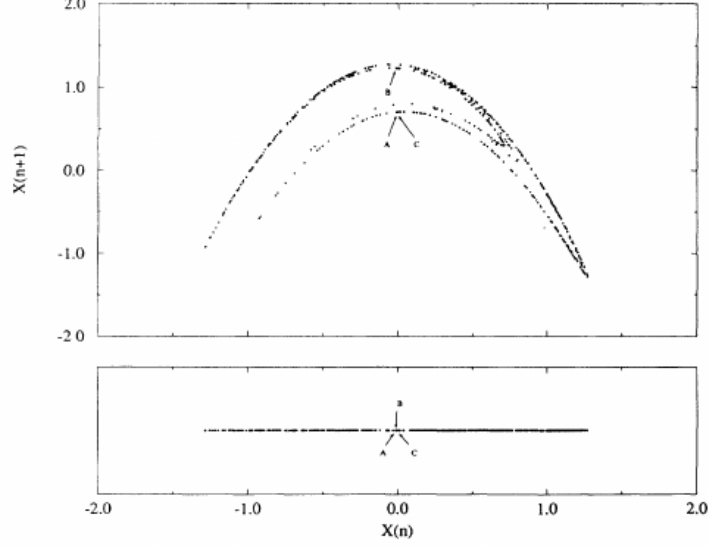
Figure 6: Schematic illustration of false neighbors. In insufficient embedding dimension (down), points A and B appear neighbors due to projection. When proper embedding is employed(up), their true separation is revealed.

1. For each point in dimension m, identify its nearest neighbor.

2. Embed the data in dimension $m + 1$.

3. Calculation the relative distance increase between each point and its former neighbor.

4. If the increase exceeds predetermined thresholds, the neighbor point is classified as a false neighbor

5. The optimal m is the smallest dimension where the fraction of false neighbors drops below an acceptable level (typically 1–5%)

Both relative and absolute criteria are included in the algorithm:

$$\text{Relative:} \quad \frac{\|\vec{y}_i^{(m+1)} - \vec{y}_j^{(m+1)}\|}{\|\vec{y}_i^{(m)} - \vec{y}_j^{(m)}\|} > R_{\text{tol}} \tag{3}$$

$$\text{Absolute:} \quad \|\vec{y}_i^{(m+1)} - \vec{y}_j^{(m+1)}\| > A_{\text{tol}} \cdot \sigma_x \tag{4}$$

where σ_x is the standard deviation of the time series.

When optimal parameters τ and m have been determined for a given signal, the phase space can be reconstructed according to Takens' theorem. This reconstruction provides the geometric picture of the underlying dynamics.

15

Figure 7 presents the reconstructed phase space for a normal EEG segment from channel 'Fp1-F7' from CHB-MIT 's chb24_01.edf data.
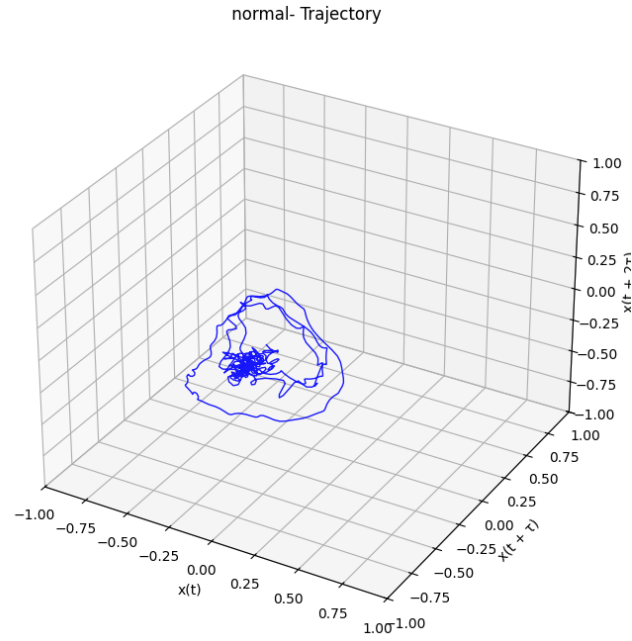

Figure 7: 3D phase space reconstruction for a 3-second EEG segment's channel.

4 Recurrence Quantification Analysis (RQA)

Having reconstructed the phase space trajectory of the EEG signals, the next step is to analyze its dynamical properties. Recurrence Quantification Analysis is a powerful nonlinear method that provides precisely this functionality by quantifying the number and duration of recurrences of a dynamical system to its previous states [37]. The core of this quantification process is the *Recurrence Plot (RP)*, a visualization which denotes the times at which the phase space trajectory revisits approximately the same area. In most non trivial cases, a phase space does not have a dimension (two or three) which allows a direct visualization, so for higher dimensional phase spaces the only solution is a projection into a two or three dimensional space. However, RP enables the examination of a higher-dimensional phase space trajectory via its two-dimensional representation of its recurrences.

4.1 The Recurrence Plot (RP)

RP is a symmetric, two-dimensional matrix that visualizes the recurrences of states. For a reconstructed trajectory $\vec{y}(t)$ of length N, the recurrence matrix $\mathbf{R}$ is defined as:

$$R_{i,j} = \Theta(\varepsilon - \|\vec{y}(i) - \vec{y}(j)\|), \quad i, j = 1, \ldots, N \tag{5}$$

where:

- $\Theta(\cdot)$ is the Heaviside step function ($\Theta(x) = 0$ if $x < 0$, and $\Theta(x) = 1$ otherwise),

- ε is a predefined distance threshold (radius),

- $\| \cdot \|$ is a norm.

By interpreting the RP several metrics can be extracted for further analysis.

5 Methodology

This section describes the two methodologies employed for processing electroencephalogram (EEG) data and performing Cross Recurrence Quantification Analysis (Cross RQA) to analyze the dynamics of epileptic and non-epileptic EEG segments.

5.1 Method A - continuous segments

The first approach($MethodA$) involves loading each EEG recording, segmenting it based on predefined boundaries and computing CRQA features for pairs of EEG channels. In the last step the mean values among all channel's combinations is calculated. The methodology is implemented in Python, utilizing libraries such as `numpy`, `matplotlib`, and `pyrqa`.

EEG data are stored in a NumPy array format (`.npy`) and accompanied by metadata containing the sampling frequency (f_s) and other relevant information. The data is loaded per specific patient's recording (f.e, patient 24 - recording number 1) from a filtered EEG file. The time axis is computed as $t = \frac{n}{f_s}$, where n is the sample index and f_s is the sampling frequency in Hertz (Hz).

The EEG data is segmented into continuous regions based on predefined boundaries according annotations (CHB-MIT dataset) that distinguish between normal and epileptic activity.

CRQA is performed to quantify the dynamical interactions among the pairs of EEG channels for each segment. The `pyrqa` library is used to compute CRQA metrics, which analyze the recurrence properties of two time series in a shared phase space. The process involves embedding the time series, computing the cross recurrence matrix, and extracting the quantitative features.

The algorithm is summarized in Algorithm 1.

For each segment and each pair of selected channels, the following steps were executed:

1. **Time Series Preparation**: For each segment, the two time series (from different channels) were truncated to the same length to ensure compatibility for CRQA computation.

2. **Parameter Estimation**: The optimal embedding dimension (m) and time delay (τ) are determined for each of the time series. The time delay is estimated using the Average Mutual Information (AMI) method, selecting the first local minimum up to a maximum lag of 25 samples. The embedding dimension is determined using the False Nearest Neighbors (FNN) method, testing dimensions up to 15, with relative and absolute tolerance parameters set to 15.0 and 2.0, respectively. The minimum of the optimal dimensions and delays from the two time series is used to ensure consistency.

Algorithm 1 Cross Recurrence Quantification Analysis (CRQA) for EEG Segments

---

1: **Input**: EEG segments $\{X_{c,i}\}$ for channels $c \in C$, segments $i = 1, \ldots, N_s$, where $N_s = 5$, number of electrodes $N_e = 3$
2: **Output**: RQA feature matrix M of shape $(N_s, N_e, N_e, 17)$
3: **for** each segment index $i = 1$ to N_s **do**
4:     **for** each channel pair $(c_1, c_2) \in C \times C$ **do**
5:         **Time Series Preparation**
6:         Truncate time series $X_{c_1,i}$ and $X_{c_2,i}$ to minimum length for compatibility
7:         **Parameter Estimation**
8:         Compute time delay τ_1 for $X_{c_1,i}$ using AMI (max lag = 25, select first local minimum)
9:         Compute time delay τ_2 for $X_{c_2,i}$ using AMI (max lag = 25, select first local minimum)
10:         Set $\tau = \min(\tau_1, \tau_2)$
11:         Compute embedding dimension m_1 for $X_{c_1,i}$ using FNN (max dimension = 15, rtol = 15.0, atol = 2.0)
12:         Compute embedding dimension m_2 for $X_{c_2,i}$ using FNN (max dimension = 15, rtol = 15.0, atol = 2.0)
13:         Set $m = \min(m_1, m_2)$
14:         **CRQA Computation**
15:         Construct cross-recurrence plot for $(X_{c_1,i}, X_{c_2,i})$ using `PyRQA` with:
16:         Fixed radius neighborhood $r = 0.1$, Euclidean metric, Theiler corrector = 1
17:         Extract 16 CRQA features: {RR, DET, L_{avg}, L_{max}, DIV, H_{diag}, LAM, TT, V_{max}, W_{avg}, W_{max}, W_{max}^{-1}, H_{vert}, H_{wvert}, DET/RR, LAM/DET}
18:         **Feature Storage**
19:         Append segment label l_i to features
20:         Store features in $M[i, c_1, c_2, :]$
21:     **end for**
22: **end for**
23: **Return** RQA feature matrix M

---

3. **CRQA Computation**: Using the `PyRQA` library, a cross-recurrence plot is constructed with a fixed radius neighborhood ($r = 0.1$) and Euclidean distance metric. The Theiler corrector is set to 1 to exclude temporally correlated points. The CRQA computation yields 16 quantitative features: recurrence rate (RR), determinism (DET), average diagonal line length (L_{avg}), longest diagonal line (L_{max}), divergence (DIV), entropy of diagonal lines (H_{diag}), laminarity (LAM), trapping time (TT), longest vertical line (V_{max}), average white vertical line length (W_{avg}), longest white vertical line (W_{max}), inverse of the longest white vertical line (W_{max}^{-1}), entropy of vertical lines (H_{vert}), entropy of white vertical lines (H_{wvert}), ratio of determinism to recurrence rate (DET/RR), and ratio of laminarity to determinism (LAM/DET).

4. **Feature Storage**: For each segment and channel pair, the 16 CRQA features are then stored in a four-dimensional matrix of shape (N_s, N_e, N_e, 17), where N_s is the number of segments in a specific recording(normal-epileptic), $N_e = 22$ is the number of electrodes, and the final dimension included the 16 features plus the segment label(normal:0 - epileptic: 1).

In order to summarize the CRQA features across electrode pairs for each EEG recording, a mean feature matrix *mean_crqa_matrix* is computed. For each segment, the 16 CRQA features were averaged across all electrode pairs, resulting in a matrix of shape (N_s, 17), where the last column retained the segment label. This mean matrix is saved for subsequent analysis, capturing the average dynamical interactions within each segment.

References

[1] Frolov, N., Maksimenko, V. and Hramov, A. (2020), Revealing a multiplex brain network through the analysis of recurrences *Chaos: An Interdisciplinary Journal of Nonlinear Science* 30(12), 121108.

[2] Recurrence quantification analysis of periodic dynamics in the default mode network in first-episode drug-naïve schizophrenia. *Psychiatry Research: Neuroimaging*, 329, 111583.

[3] Recurrence quantification analysis of rs-fMRI data: A method to detect subtle changes in the TgF344-AD rat model. *Computer Methods and Programs in Biomedicine*, 257, 108378.

[4] Lameu, E. L., Yanchuk, S., Macau, E. E. N., Borges, F. S., Iarosz, K. C., Caldas, I. L., Protachevicz, P. R., Borges, R. R., Viana, R. L., Szezech, J. D., Batista, A. M. and Kurths, J. (2018). Recurrence quantification analysis for the identification of burst phase synchronisation. *Chaos: An Interdisciplinary Journal of Nonlinear Science*, *28*(8), 085701. https://doi.org/10.1063/1.5024324

[5] Lombardi, A., Guccione, P. and Mascolo, L. (2014). Analysis of fMRI data using the complex systems approach. In *20th IMEKO TC4 International Symposium and 18th International Workshop on ADC Modelling and Testing* (pp. 293-298). Benevento, Italy.

[6] Pitsik, E. (2025). Recurrence quantification analysis and theta-band functional networks detect age-related changes in brain sensorimotor system: VR-based approach. *The European Physical Journal Special Topics.* https://doi.org/10.1140/epjs/s11734-025-01509-y

[7] Guglielmo, G., Wiltshire, T. J. and Louwerse, M. (2022). Training machine learning models to detect group differences in neurophysiological data using recurrence quantification analysis based features. *ICAART 2022 - 14th International Conference on Agents and Artificial Intelligence*, 430-434.

[8] Lopes, M. A., Zhang, J., Krzeminski, D., Hamandi, K., Chen, Q., Livi, L. and Masuda, N. (2020). Recurrence quantification analysis of dynamic brain networks. *European Journal of Neuroscience*, 00, 1-20. https://doi.org/10.1111/ejn.14960

[9] Pentari, A., Tzagkarakis, G., Tsakalides, P., Simos, P., Bertstas, G., Kavroulakis, E., Marias, K., Simos, N. J. and Papadaki, E. (2022). Changes in resting-state functional connectivity in neuropsychiatric lupus: A dynamic approach based on recurrence quantification analysis. *Biomedical Signal Processing and Control, 72*, 103285. https://doi.org/10.1016/j.bspc.2021.103285

[10] Pentari, A., Simos, N., Tzagarakis, G., Kagialis, A., Bertsias, G., Kavroulakis, E., Gratsia, E., Sidiropoulos, P., Boumpas, D. T. and Papadaki, E. (2023). Altered hippocampal connectivity dynamics predicts

memory performance in neuropsychiatric lupus: A resting-state fMRI study using cross-recurrence quantification analysis. *Lupus Science & Medicine*, *10*(1), e000920. https://doi.org/10.1136/lupus-2023-000920

[11] Gruszczyńska, I., Mosdorf, R., Sobaniec, P., Żochowska-Sobaniec, M. and Borowska, M. (2019). Epilepsy identification based on EEG signal using RQA method. *Advances in Medical Sciences*, 64(1), 58-64. https://doi.org/10.1016/j.advms.2018.08.003

[12] Mo, J., Zhang, J., Hu, W., Wang, X., Zhao, B., Zhang, K. and Zhang, C. (2022). Neural underpinnings of default mode network on empathy revealed by intracranial stereoelectroencephalography. *Psychiatry and Clinical Neurosciences, 76*(12), 659-666. https://doi.org/10.1111/pcn.13470

[13] Vanithamani Palanisamy, A. Ranichitra, and Radhamani Ellapparaj, A differential biomarker based on recurrence quantification analysis of EEG signal and genetic algorithm for epilepsy diagnosis. *Journal of Artificial Intelligence and System Modelling*, 2(2):74–85, 2024. 10.22034/jaism.2024.450400.1046

[14] Ngamga, E. J., Bialonski, S., Marwan, N., Kurths, J., Geier, C. and Lehnertz, K. (2016). Evaluation of selected recurrence measures in discriminating pre-ictal and inter-ictal periods from epileptic EEG data. *Physics Letters A*, *380*(16), 1419–1425. https://doi.org/10.1016/j.physleta.2016.02.024

[15] Fan, M. and Chou, C.-A. (2019). Detecting abnormal pattern of epileptic seizures via temporal synchronization of EEG signals. *IEEE Transactions on Biomedical Engineering*, 66(3), 601-608. https://doi.org/10.1109/TBME.2018.2850959

[16] P. Núñez, J. Poza, C. Gómez, V. Barroso-García, A. Maturana-Candelas, M. A. Tola-Arribas, M. Cano, and R. Hornero, Characterization of the dynamic behavior of neural activity in Alzheimer's disease: exploring the non-stationarity and recurrence structure of EEG resting-state activity, *Journal of Neural Engineering*, vol. 17, no. 1, p. 016071, 2020, doi: https://doi.org/10.1088/1741-2552/ab71e9.

[17] Yang, C., Luan, G., Liu, Z. and Wang, Q. (2019). Dynamical analysis of epileptic characteristics based on recurrence quantification of SEEG recordings. *Physica A: Statistical Mechanics and its Applications*, *523*, 507–515. https://doi.org/10.1016/j.physa.2019.02.017

[18] Rangaprakash, D. (2014). Connectivity analysis of multichannel EEG signals using recurrence based phase synchronization technique. *Computers in Biology and Medicine, 46*, 11-21. https://doi.org/10.1016/j.compbiomed.2013.10.025

[19] Trulla, L. L., Giuliani, A., Zbilut, J. P., and Webber, C. L., "Recurrence Quantification Analysis of the Logistic Equation with Transients," *Physics Letters A*, vol. 223, no. 4-5, pp. 255–260, 1996. `doi: 10.1016/S0375-9601(96)00741-4`

[20] Webber, C. L. and Zbilut, J. P., "Recurrence Quantification Analysis of Nonlinear Dynamical Systems," in *Tutorials in Contemporary Nonlinear Methods for the Behavioral Sciences*, pp. 26–94, 2005.

[21] Thomasson, N., Hoeppner, T. J., Webber, C. L., and Zbilut, J. P., "Application of Recurrence Quantification Analysis to EEG Signals," *International Journal of Computer Research*, 2002.

[22] Marwan, N., Schinkel, S., and Kurths, J., "Recurrence Plots 25 Years Later – Gaining Confidence in Dynamical Transitions," *EPL (Europhysics Letters)*, vol. 101, no. 2, p. 20007, 2013. `doi: 10.1209/0295-5075/101/20007`

[23] Heunis, T., Aldrich, C., Peters, J. M., Jeste, S. S., Sahin, M., Scheffer, C., and de Vries, P. J., "Recurrence quantification analysis of resting state EEG signals in autism spectrum disorder – a systematic methodological exploration of technical and demographic confounders in the search for biomarkers," *BMC Medicine*, vol. 16, no. 1, p. 101, 2018.

[24] Eckmann, J.-P., Kamphorst, S. O. and Ruelle, D. (1987). Recurrence plots of dynamical systems. *Europhysics Letters*, *4*(9), 973–977.

[25] Timothy, L. T., Krishna, B. M. and Nair, U. (2017). Classification of mild cognitive impairment EEG using combined recurrence and cross recurrence quantification analysis. *International Journal of Psychophysiology*, *120*, 86–95. https://doi.org/10.1016/j.ijpsycho.2017.07.006

[26] Kashyap, A. and Keilholz, S. (2019). Dynamic properties of simulated brain network models and empirical resting-state data. *Network Neuroscience,* *3*(2), 405-426. https://doi.org/10.1162/netn_a_00070

[27] Carrubba, S., Frilot, C. and Marino, A. A. (2019). Optimization of recurrence quantification analysis for detecting the presence of multiple sclerosis. *Journal of Medical and Biological Engineering*, *39*(6), 806–815. https://doi.org/10.1007/s40846-019-00462-1

[28] Shalbaf, R., Behnam, H., Sleigh, J. W., Steyn-Ross, D. A., & Steyn-Ross, M. L. (2014). Frontal–temporal synchronization of EEG signals quantified by order patterns cross recurrence analysis during propofol anesthesia. *IEEE Transactions on Neural Systems and Rehabilitation Engineering*, 22(6), 1164–1174. https://doi.org/10.1109/TNSRE.2014.2350537

[29] Jiang, X., Bian, G.-B., and Tian, Z. (2019). Removal of Artifacts from EEG Signals: A Review. Sensors, 19(5), 987. https://doi.org/10.3390/s19050987

[30] Dhanaseivam, P. S., and Chellam, C. N. (2023). A review on preprocessing of EEG signal. In *2023 9th International Conference on Biosignals, Images and Instrumentation (ICBSII 23)*. Madurai, India.

[31] Jiang, X., Bian, G.-B., and Tian, Z. (2019). Removal of artifacts from EEG signals: A review. *Sensors, 19*(5), 987. https://doi.org/10.3390/s19050987

[32] Sen, D., Mishra, B. B., and Pattnaik, P. K. (2023). A review of the filtering techniques used in EEG signal processing. In *Proceedings of the 7th International Conference on Trends in Electronics and Informatics (ICOEI 2023)* (pp. 270–278). Bhubaneshwar, India.

[33] Mihajlović, D. (2019). EEG Spectra vs Recurrence Features in Understanding Cognitive Effort. *In Proceedings of the 2019 International Symposium on Wearable Computers (ISWC '19)*, September 9–13, 2019, London, United Kingdom. ACM, New York, NY, USA, 6 pages. https://doi.org/10.1145/3341163.3347746

[34] Takens, F. (1981). Detecting strange attractors in turbulence. In *Lecture Notes in Mathematics* (Vol. 898, pp. 366-381). Springer.

[35] Kennel, M. B., Brown, R., & Abarbanel, H. D. I. (1993). Determining embedding dimension for phase-space reconstruction using a geometrical construction. *Physical Review A*, 45(6), 3403–3411.

[36] Fraser, A. M., & Swinney, H. L. (1986). Independent coordinates for strange attractors from mutual information. *Physical Review A, 33*(2), 1134–1140. https://doi.org/10.1103/PhysRevA.33.1134

[37] Marwan, N., Carmen Romano, M., Thiel, M., & Kurths, J. (2007). Recurrence plots for the analysis of complex systems. *Physics Reports, 438(5–6)*, 237–329. https://doi.org/10.1016/j.physrep.2006.11.001

[38] Marwan, N. (2003). Encounters with neighbours: Current developments of concepts based on recurrence plots and their applications (*Doctoral dissertation, University of Potsdam, Germany*). Institut für Physik, Universität Potsdam.

[39] Berényi, A., Kurics, T., Bence, M., Németh, M., Laszlov'szky, T., Nádasdi, M., Ráfi, P., Vincze, V. and Högye, S. *Systems and Methods for Seizure Detection and Closed-Loop Neurostimulation*. U.S. Patent Application No. US 2025/0195894 A1, filed December 13, 2024, published June 19, 2025.

[40] Zhongnan, Z. and Weizhen, L. (2018)*An EEG signal classification model based on genetic algorithm and random forest*, Chinese Patent CN108615024A, Applicant: Xiamen University.

[41] Chen, Y., Hao, H., & Li, L. (2019). *Implantable closed-loop deep brain stimulation system* (Patent No. CN106512206B). State Intellectual Property Office of the People's Republic of China.